Available online at www.sciencedirect.com
SCIENCE DIRECT
Thin Solid Films 473 (2005) 236–240
thin solid films
www.elsevier.com/locate/tsf

Spontaneous oxide reduction in metal stacks

Wentao Qin[a,*], Alex A. Volinsky[b], Dennis Werho[a], N. David Theodore[a], Mike Kottke[a], Chandra Ramiah[c]

[a]Advanced Products R&D Lab., Freescale Semiconductor Inc., Tempe, AZ 85284, USA
[b]Department of Mechanical Engineering, University of South Florida, Tampa, FL 33620, USA
[c]RF/IF Device Engineering, Freescale Semiconductor Inc., Tempe, AZ 85284, USA

Received 16 June 2003; received in revised form 19 July 2004; accepted 19 July 2004
Available online 15 September 2004

Abstract

Aluminum and copper interconnects are widely used for microelectronic applications. A problem can arise when interfacial oxides are present. Such oxides can significantly degrade device performance by increasing electrical resistance. This paper describes analyses of interfacial oxide layers found in Al/Ta and Ta/Cu metal stacks. The analyses were performed through transmission electron microscopy (TEM). The data indicated that the interfacial oxides resulted from spontaneous reductions; that is, Al spontaneously reduced Ta_2O_5 to form Al_2O_3, while Ta spontaneously reduced Cu oxide to form Ta_2O_5.

PACS: 82.65.Dp; 68.35; 73.90.+f; 61.16.Bg; 82.80.Pv
Keywords: Spontaneous oxide reduction; Interfaces; Transmission electron microscopy; Spectrum profile; Energy-dispersive spectroscopy; Electron energy-loss spectroscopy; Oxidation; Metallization

1. Introduction

Modern microelectronic manufacturing relies on the use of advanced metallization schemes. Although the industry has made a switch from Al/SiO_2 to Cu/low-k dielectric metallization, there remain certain applications which require Al to be present in the device. For example, it is sometimes advantageous to use Al for metallization top layers in order to protect the underlying Cu from oxidation, as well as to make the process compatible with existing wire-bonding and packaging schemes.

In the metallization process, surface oxidation of individual films can lead to further reactions, which will ultimately affect physical properties of the stack, such as the electrical resistance, wettability and adhesion. Some of the changes are favorable to device performance, while others are detrimental. Therefore, it is important to understand, control and even utilize such oxidation and reactions.

Both Al and Ti have higher affinities for oxygen than Si does; consequently, when either Al or Ti is deposited on SiO_2, the metal can reduce the underlying SiO_2 [1–6]. A similar observation has been made from metal/metal oxide interfaces in powders [7].

Reduction of surface oxides has been found to correlate with wettability, and eventually adhesion, in different metal/metal oxide systems [8,9]. For instance, metals with higher affinities to oxygen showed higher wettability and increased adhesion in the case of metal–TiO interfaces [10].

This paper reports analyses of interfacial oxides in Al/Ta and Ta/Cu stacks, with discussion of the corresponding spontaneous oxide reductions based on thermodynamics. The physical properties of concern are the electrical resistances of the stacks; therefore, process modifications to remove the interfacial oxides and thereby to significantly reduce the electrical resistances of the stacks are also mentioned.

* Corresponding author.
E-mail address: Wentao.Qin@Freescale.com (W. Qin).

0040-6090/$ - see front matter © 2004 Elsevier B.V. All rights reserved.
doi:10.1016/j.tsf.2004.07.066

2. Experimental details

Two metal film stacks, one Al/Ta and the other Ta/Cu, were deposited separately on Si wafers. In the case of the Al/Ta stack, the deposition of Ta was followed by an exposure to the air during transfer of the wafer to a different tool for the deposition of Al. The Ta film surface was not sputter cleaned prior to the Al deposition.

In the case of the Ta/Cu stack, the Cu film was photolithographically patterned. The photoresist used for the patterning was then stripped off with an oxygen plasma ashing process, which caused surface oxidation of the Cu film. A radiofrequency (RF) sputter clean was therefore implemented in order to remove the surface oxide from the Cu film, prior to the deposition of Ta. The strength (power and duration) of the RF sputter clean was equivalent to that of a process used to remove 10 nm of SiO_2.

Cross-section transmission electron microscopy (TEM) analyses were performed to investigate the Al/Ta and Ta/Cu interfaces in the two stacks. A focused ion beam (FIB) pre-thin method was used to prepare the TEM samples. In the preparation, a 3-mm wide and 10-μm-thick slice containing the area of interest was obtained from the wafer through cleaving and mechanical grinding. The slice was then glued to a Mo half-washer, and the area of interest was finally thinned down to electron translucency with a dual-beam FIB tool.

The TEM used is equipped with a field-emission gun, and operates at an accelerating voltage of 200 kV. Imaging was performed with parallel illumination. Elemental analyses were carried out via energy-dispersive spectroscopy (EDS) and parallel electron energy-loss spectroscopy (PEELS). Both of these elemental analysis techniques were applied in scanning transmission electron microscopy (STEM) mode. In the STEM mode, the electron beam was focused to a fine probe with a full-width-at-half-maximum (FWHM) on the order of 1 nm, i.e., a nanoprobe. Electrons in the nanoprobe interacted with materials in the area of interest, which generated characteristic signals that were acquired for the analyses. Fig. 1 is an image of a nanoprobe, whose FWHM is equal to 1.4 nm.

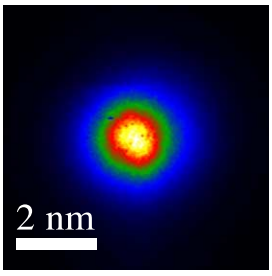

Fig. 1. An image of a nano-probe that could be used for elemental and chemical bonding analyses of features on the nanometer scale. The FWHM of the probe is 1.4 nm.

3. Results and discussion

3.1. Spontaneous reduction of Ta oxide by Al

A high-resolution TEM image, obtained from the Al/Ta stack, is shown in Fig. 2. The image reveals the presence of a 3- to 5-nm amorphous layer between the Ta and the Al layers.

Fig. 3 shows EDS spectra, one acquired from the Al layer, and the second from the interfacial layer. Both Al and O K_α peaks are evident. The Si K_α peaks in the spectra arose from Si/SiO_2 redeposited on both sides of the TEM sample during FIB sample preparation. Fluorescence of Si in both the substrate and SiO_2 interlayer dielectric (ILD) also contributed to the Si signal. The spectra indicate that the interfacial layer is Al oxide. After subtraction of O K_α components from the background (mainly arising from excitation of O in the SiO_2 ILD by Bremsstrahlung X-rays and uncollimated electrons) and the redeposited SiO_2, the interfacial layer was calculated to consist of 41 at.% of Al and 59 at.% of O [11,12]. Therefore, the stoichiometry of the interfacial oxide, as inferred from EDS quantification, is Al_2O_3.

In addition to basic elemental information from EDS, chemical bonding information was acquired from Energy Loss Near-Edge Structure (ELNES) at the Al K ionization edge PPELS. Presented in Fig. 4 are PEELS spectra acquired from the interfacial layer and from a site in the Al layer about 3 nm above the interfacial layer. The presence of the sharp feature in the $L_{2,3}$ edges of Al indicates that the Al atoms in the interfacial layer have been oxidized to form Al_2O_3 [13].

The above results can be interpreted based on thermodynamics. During the wafer transfer, the Ta film surface was oxidized to form Ta oxide. Al was subsequently deposited on this oxidized surface. Thermodynamically, Al can reduce the surface Ta oxide through a spontaneous reaction, as shown below:

$$10Al + 3Ta_2O_5 \rightarrow 5Al_2O_3 + 6Ta,$$
$$\Delta F = -489K \text{ Cal/mol at } 25^\circ C \quad [14], \qquad (1)$$

because the free energy of the reaction is negative. Eq. (1) represents the mechanism for the majority of the oxide layer reduction. This is because most of the native oxides (~85%) formed on Ta metal are Ta_2O_5, while the remainder are present as suboxides, as indicated by X-ray photoelectron spectroscopy (XPS) analyses carried out both in our lab and elsewhere [15]. The suboxides of Ta are not well characterized and there is some dispute as to their compositions. Some evidence indicates that these suboxides are in the (+1) and (+3) oxidation states [16], which would suggest compounds of Ta_2O and Ta_2O_3. However, other evidence indicates oxidation states of (+2) and (+4), suggesting compounds of TaO and TaO_2 [17]. Our XPS analyses indicate that two suboxides were present on the Ta metal, but it is not clear exactly which ones of those suggested above were present. No comment is provided here concerning the

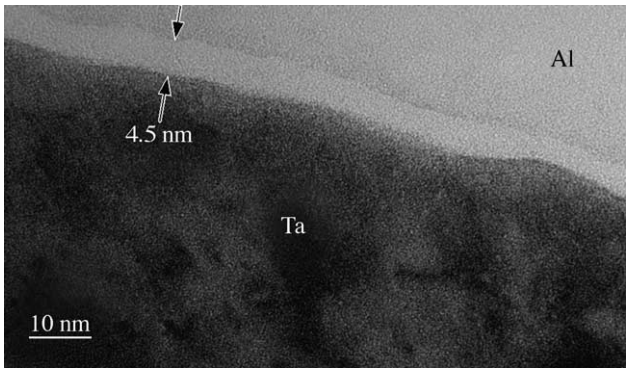

Fig. 2. High-resolution cross-section TEM image of the Ta/Al metal stack. A 3–5 nm amorphous oxide layer is present between Ta and Al.

reduction of other suboxides by Al, due to unavailability of the associated free energies in the literature.

The presence of interfacial oxide, be it Ta-based or Al-based, would increase electrical resistance of the stack.

3.2. Spontaneous reduction of Cu oxide by Ta

A high-resolution TEM image obtained from the Ta/Cu stack is shown in Fig. 5. The image reveals the presence of a 3- to 4-nm interfacial layer, suggesting that the pre-Ta RF sputter clean did not completely remove the surface Cu oxide. EDS and PEELS spectrum profiling were performed simultaneously across the interfacial layer. Fig. 6 shows profiles of the areal densities of O and Cu, projected along the electron transmission direction, and the integrated intensities of the Ta L_α X-ray peak. The areal density was calculated through the following formula of

$$N = \frac{I_k(\beta, \Delta)}{I(\beta, \Delta)\sigma_k(\beta, \Delta)} \tag{2}$$

without taking $\sigma_k(\beta, \Delta)$ into account, as it is constant throughout the profile [18]. In this expression, N is the areal density, $I_k(\beta, \Delta)$ is the core loss integral including plural scattering, $I(\beta, \Delta)$ is the low-loss intensity integral, β is the

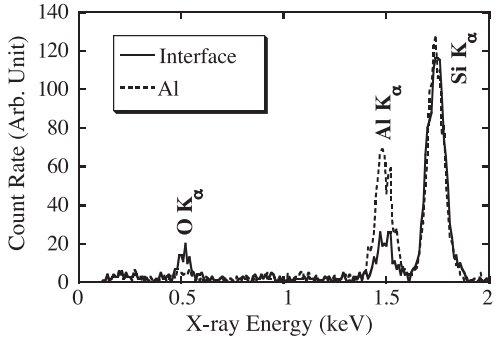

Fig. 3. EDS spectra obtained from the Al–Ta interfacial layer and an Al area immediately above the interface. The Si peaks arose from Si/SiO_2 redeposited on both sides of the TEM sample during FIB sample preparation, as well as from fluorescence of Si that is present in both substrate and SiO_2 interlayer dielectric in the sample. The spectra indicate that the interfacial layer material is Al oxide.

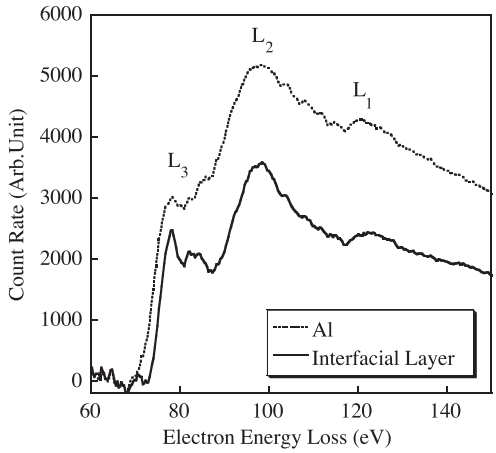

Fig. 4. Electron energy loss spectra (EELS) acquired from the Al–Ta interfacial layer shown in Fig. 2 and an Al area about 3 nm above the interfacial layer. The presence of the sharp feature at the $L_{2,3}$ edges of Al indicates that the Al atoms in the interfacial layer have been oxidized to from Al_2O_3 [13].

collection angle, Δ is the energy range over which integration of electron intensity is performed and $\sigma_k(\beta, \Delta)$ is a partial ionization cross-section for energy losses within Δ from the ionization threshold.

It can be seen that with the electron beam positioned at the center of the interfacial layer, there is no Cu $L_{2,3}$ edge detected, in both Figs. 6 and 7. Fig. 7 shows PEELS spectra acquired from the interfacial layer and from a site about 6 nm below the interfacial layer and in the acquired from the same two sites, in the energy range of the Cu $L_{2,3}$ edges. Fig. 8 shows EDS spectra, the first obtained with the electron beam positioned at the center of the interfacial layer and the second obtained from a site 6 nm immediately below the interface in the Cu layer. EDS quantification yields 65 at.% for O and 36 at.% for Ta.

Among the three phases of Ta oxide (Ta_2O_5 and the two suboxides), Ta_2O_5 is known to be much more stable than the

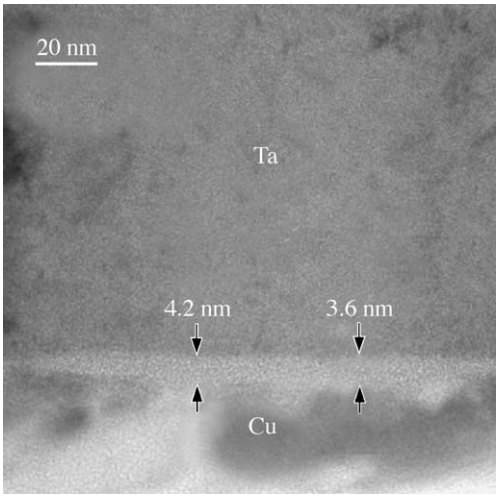

Fig. 5. High-resolution cross-section TEM image the Ta/Cu metal stack showing a 3- to 5-nm-thick interfacial Ta oxide layer which formed through a spontaneous reduction of a surface Cu oxide layer by Ta.

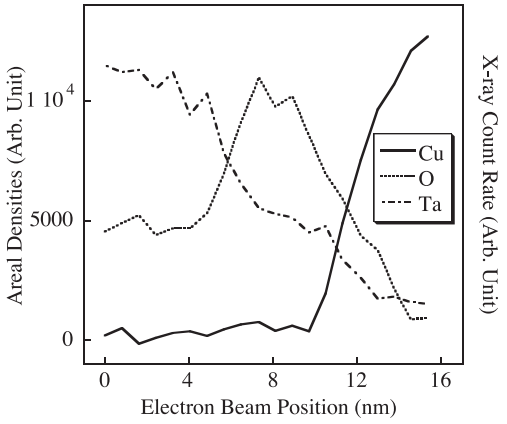

Fig. 6. Profiles of areal densities of Cu and O based on integrated intensities of the Cu $L_{2,3}$ edges and O K edge, and profile of the integrated intensities of Ta Lα X-rays.

other two and to be more difficult to reduce [17]. As previously discussed, native oxides on Ta films have been found to consist predominantly of Ta_2O_5 together with other suboxides [17]. Considering this information in conjunction with our experimental data, it is reasonable to infer that the surface Cu oxide was reduced spontaneously by the Ta and that the reaction produced Ta oxides, which consist at least primarily of Ta_2O_5, with possible inclusion of other Ta oxides. The only two reduction reactions, where the free energies are available in the literature, were both found to be spontaneous [14]. The reactions are:

$$2Ta + 5Cu_2O \rightarrow Ta_2O_5 + 10Cu, \quad \Delta F = -272K \text{ Cal/mole at } 25^\circ C \tag{3}$$

$$2Ta + 5CuO \rightarrow Ta_2O_5 + 5Cu, \quad \Delta F = -120K \text{ Cal/mole at } 25^\circ C \tag{4}$$

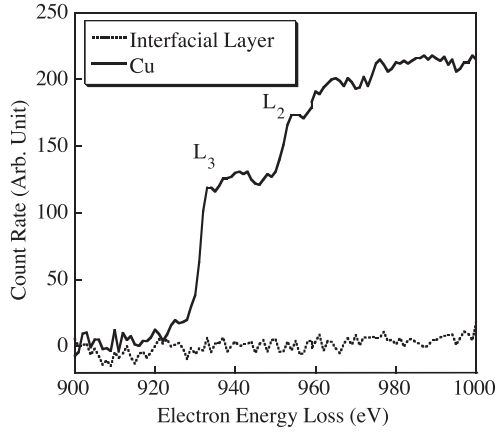

Fig. 7. Electron energy loss spectra acquired with the electron beam positioned in the middle of the interfacial layer and a site 6 nm immediately below in the Cu layer. Cu $L_{2,3}$ edges are absent in the first spectrum, indicating the Cu in the middle of the interfacial layer was below the detection limit. This observation supports the interpretation that the weak X-ray Cu Lα peak in Fig. 8 arose from fluorescence.

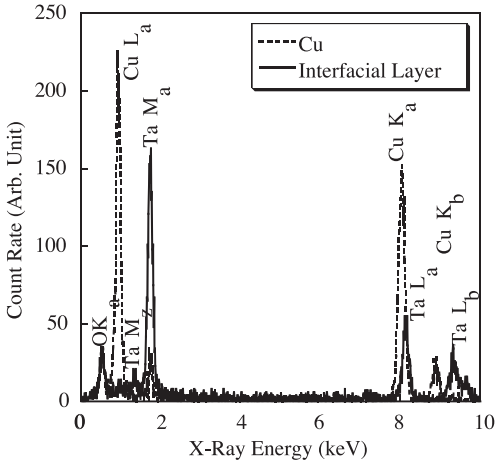

Fig. 8. EDS spectra obtained with the electron beam positioned at the center of the Ta–Cu interfacial layer and a site 6 nm immediately below the interface in the Cu layer. The interfacial layer is Ta oxide. EDS quantification indicates that atomic percentages are 35% for Ta and 65% for O.

The possibility of other reactions, in which suboxides of Ta are produced, was not evaluated at this point due to the unavailability of their free energies in the literature. Independent of specific reductions of surface oxides, the presence of any oxide layer is expected to increase the electrical resistance of the stack.

3.3. Process optimization

Increased metallization resistance is a problem for circuit applications and needs to be solved. Efforts made to return the resistance of the Al/Ta stack to a normal value are briefly mentioned as follows. One solution to this problem is to remove the surface oxide that is present on the Ta film, by an RF sputter clean before the Al sputter deposition. A high-resolution TEM image of the Al–Ta interface processed with this modification is presented in Fig. 9. The

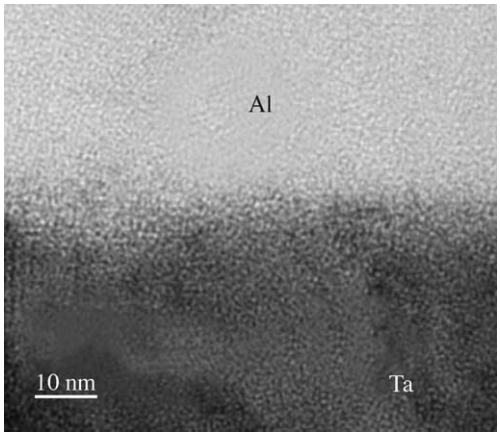

Fig. 9. High-resolution TEM image of the Al–Ta interface after a pre-Al sputter was implemented. The sputter clean removed the surface oxide on Ta resulting from the air exposure. The image shows that there is no longer any interfacial oxide.

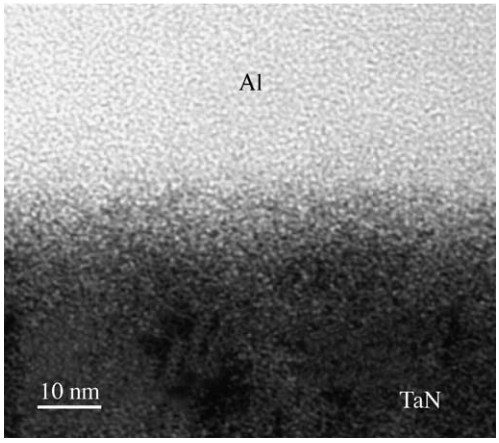

Fig. 10. High-resolution TEM image of the Al-TaN interface. The deposition of Al and TaN were carried out in the same deposition tool, eliminating air exposure of the water between the depositions. Consequently, there was no interfacial oxide present in the stack.

image shows that there is no longer any interfacial oxide within the stack.

Another solution to the problem was to replace Ta with TaN, which could be deposited in the same deposition chamber as the Al. This solution eliminated any exposure of the wafer surface to air prior to deposition of the Al. A high-resolution TEM image of the Al–TaN interface from such a wafer is presented in Fig. 10. The image, again, shows the absence of any interfacial oxide. Electrical tests on the stack after both optimizations showed that the electrical resistance had been reduced to about 1/10 of the value measured before the process optimizations.

4. Conclusions

Interfacial oxide layers in stacks containing adjacent thin films of Al and Ta, and Ta and Cu, resulted in elevated resistances. Surface oxides formed during an air exposure of the Ta film in the first stack, and during an ash to remove photoresist, which was followed by an insufficient pre-Ta sputter, in the second stack. The interfacial oxide layers experienced reduction of Ta oxide by Al, and reduction of Cu oxide by Ta. The oxide layers were observed and analyzed through brightfield imaging, EDS and PEELS in TEM. As an example of process optimization, resistance of the Al/Ta stack was reduced to acceptable values by removal of surface Ta oxide with a pre-Al sputter, or, alternatively, by replacing the Ta with TaN, which could be deposited in the same chamber as Al without any air exposure.

Acknowledgements

The authors are grateful to Susan Williamson and Lorraine Johnston for TEM sample preparation, to Mark DeHerrera, Greg Grynkewich and Brian Butcher for processed wafers, and to Dr. Peter Fejes and Dr. Joe Kulik for valuable discussions concerning EDS and PEELS analyses.

References

[1] C.R.M. Grovenor, Microelectronic Materials, IOP Publishing, Philadelphia, PA, 1989, p. 239.
[2] S.P. Murarka, M.C. Peckerar, Electronic Materials: Science and Technology, Academic Press, San Diego, CA, 1989, p. 284.
[3] L.M. Koschier, S.R. Wenham, Record of the Twenty-Eighth IEEE Photovoltaic Specialists Conference—2000, IEEE, Piscataway, NJ, USA, 2000, p. 407.
[4] M.A. Taubenblatt, C.R. Helms, J. Appl. Phys. 53 (9) (1982) 6308.
[5] M. Liehr, F.K. LeGoues, G.W. Rubloff, P.S. Ho, J. Vac. Sci. Technol., A 3 (3) (1985) 983.
[6] T. Ohwaki, K. Aoki, T. Yoshida, S. Hashimoto, Y. Mitsushima, Y. Taha, Surf. Sci. 496 (1999) 433.
[7] Ch. Laurent, Ch. Blaszczyk, M. Brieu, A. Rousset, Nanostruct. Mater. 6 (1995) 317.
[8] Yu.V. Naidich, Prog. Surf. Membr. Sci. 14 (1981) 353.
[9] D.M. Lipkin, J.N. Israelachvili, D.R. Clarke, Philos. Mag., A 76 (1997) 715.
[10] U. Diebold, J-M. Pan, T.E. Madey, Surf. Sci. 333 (1995) 845.
[11] G. Cliff, G. Lorimore, J. Microsc. 103 (1975) 203.
[12] D. Joy, in: D. Joy, A. Romig Jr., J. Goldstein (Eds.), Principles of Analytical Electron Microscopy, Plenum Press, New York, 1986, p. 155.
[13] C. Ahn, O. Krivanek, EELS Atlas, Arizona State University High-Resolution Electron Microscopy Facility and Gatan, 1983.
[14] L.F. Epstein, Ceram. Age (1954 April) 37.
[15] B.V. Crist, Monochromatic XPS Spectra: The Elements and Native Oxides, Wiley, Chichester, 2000, p. 478.
[16] F.J. Himpsel, J.F. Morar, F.R. McFeely, R.A. Pollak, Phys. Rev., B 30 (12) (1984) 7236.
[17] N.N. Greenwood, A. Earnshaw, Chemistry of the Elements, Butterworth-Heinemann, Oxford, 1997, p. 981.
[18] R. Egerton, Electron Energy-Loss Spectroscopy in the Electron Microscope, Plenum Press, New York, 1996, p. 280.